

Solubilities of Cerium(IV), Terbium(III), and Iron(III) β -Diketonates in Supercritical

Carbon Dioxide*

Wendy C. Andersen,[†] Robert E. Sievers,[†] Anthony F. Lagalante,[‡] and Thomas J.**

Bruno[‡]

[†] Department of Chemistry and Biochemistry, University of Colorado, Boulder, CO 80309

[‡] Chemical Science and Technology Laboratory, National Institute of Standards and
Technology, 325 Broadway, Boulder, CO 80303

** Author to whom correspondence should be addressed. FAX: (303) 492-1414, E-mail:
rosella@terra.colorado.edu

* Contribution of the United States Government. Not subject to copyright in the United
States.

Abstract

The solubilities of the cerium(IV), terbium(III), and iron(III) chelates of the anions of 2,2,7-trimethyl-3,5-octanedionate H(tod), 2,2,6,6-tetramethyl-3,5-octanedionate H(thd), and 2,4-pentanedionate H(acac) were measured in supercritical carbon dioxide by near infrared spectroscopy from 313 to 333 K and 10 to 35 MPa with a high-pressure optical cell. Solubilities increased in the order $\text{acac} < \text{thd} < \text{tod}$ for all metal β -diketonates, with $\text{Ce}(\text{tod})_4$, $\text{Tb}(\text{tod})_3$, and $\text{Fe}(\text{tod})_3$ an order of magnitude more soluble than $\text{Ce}(\text{thd})_4$, $\text{Tb}(\text{thd})_3$, and $\text{Fe}(\text{acac})_3$, respectively. For the larger metal ions, Ce^{4+} and Tb^{3+} , the flexibility of the isobutyl group in the tod ligand creates a more lipophilic shell around the central metal ion, increasing the solubility of the chelate in CO_2 . These observations indicate that the isobutyl group is at least as CO_2 -philic as the *tert*-butyl moiety. The experimental solubilities were correlated using the model proposed by Chrastil. Finally, Ce^{4+} , Tb^{3+} , and Fe^{3+} were extracted from aqueous solutions using H(tod) dissolved in supercritical CO_2 .

Introduction

Supercritical fluid extraction (SFE) with carbon dioxide has been proposed as an environmentally benign extraction process for analytical to industrial-scale separations in fields as varied as environmental analysis and consumer product processing. The use of supercritical CO_2 containing chelating agents is an attractive technique for the remediation of metal-contaminated wastes or the extraction of high-value metals because the metal is both removed and concentrated in the precipitated extract, eliminating the need for

additional concentration steps. β -diketone ligands form a lipophilic shell around metal ions, enabling the dissolution of the metal chelate in non-polar supercritical CO₂. As a result, these chelating agents have been widely used to extract metal ions from a variety of sample matrixes using SFE.¹⁻³ For metal extraction, accurate solubility data for the metal β -diketonate complex in CO₂ is crucial for designing efficient SFE methods. While the solubilities of many metal chelates have been measured in supercritical CO₂,^{4, 5} some of the most promising and inexpensive chelates have not yet been studied.

In the current study, the solubilities of cerium(IV), terbium(III), and iron(III) β -diketonate complexes with the ligands 2,2,7-trimethyl-3,5-octanedione H(tod), 2,2,6,6-tetramethyl-3,5-heptanedione H(thd), and 2,4-pentanedione H(acac) were determined. The solubilities were measured spectroscopically in supercritical CO₂ from 313 to 333 K and from 10 to 35 MPa by a static near infrared (NIR) method. NIR is particularly well suited for measuring the absorbance of highly colored (or colorless) metal chelates that have prohibitively high (or low) absorptivities in the ultraviolet and visible regions. In addition, molar absorptivities in the NIR do not show a strong dependence on the density of the supercritical fluid, as is the case in the UV-visible spectra.⁶ The solubility data were interpreted with respect to the structure of these metal chelates and correlated with the empirical model proposed by Chrastil.⁷

While extractions using fluorinated β -diketonates are more frequently encountered in the SFE literature, non-fluorinated chelating agents are substantially less expensive, providing an economically feasible option for industrial-scale operations. Ce(IV), Tb(III), and Fe(III), surrogates for tri- and tetravalent actinides, were extracted from aqueous

solutions using H(tod) and supercritical CO₂ at 333 K and 20.3 MPa to evaluate the feasibility of using H(tod) in SFE of radioactive waste.

Experimental

Chemicals. SFC grade carbon dioxide was used as received from a commercial supplier. Ce(thd)₄, Tb₂(thd)₆, Fe(thd)₃, Fe(acac)₃, (NH₄)₂Ce(NO₃)₆, Tb(NO₃)₃•6H₂O, FeCl₃•6H₂O, and sodium acetate were purchased from commercial suppliers. All chemicals were used as received; however, disparate solubility results were initially found for Tb₂(thd)₆ and Fe(thd)₃ and led us to further purify these compounds by heating for two hours under vacuum (388 and 353 K, respectively) to remove a possible free ligand impurity. Ce(tod)₄, Tb₂(tod)₆, Fe(tod)₃, and H(tod) were synthesized and purified according to methods in the literature.^{8,9} Although solid Tb₂(tod)₆ and Tb₂(thd)₆ are dimeric, the monomers are obtained by dissolution in organic solvents.⁸

Solubility Apparatus. The solubility measurement apparatus consisted of a high-pressure syringe pump, NIR spectrophotometer, optical cell with thermostat, and pressure transducer (Figure 1). A commercial scanning UV-visible-NIR spectrophotometer was used for all experiments, set for 4.0 nm resolution and a scan speed of 2000 nm/min. The optical cell was custom built from 316 stainless steel and was fitted with sapphire windows (0.64 cm thick) sealed with polyetheretherketone (PEEK) gaskets. A cavity at the bottom of the cell accommodated a Teflon-coated magnetic stirring bar, coupled to an external magnetic stirring device. The cell had a pathlength of 3.93 ± 0.06 cm and an internal volume of 2.80 ± 0.01 mL. The entire cell was thermostatted in an aluminum block by four cartridge heaters. A platinum resistance temperature sensor was used to measure and

control the temperature to within ± 0.1 K using a microprocessor based temperature controller. The cell pressure was monitored *in-situ* to within $\pm 1\%$ by a pressure transducer calibrated using a deadweight pressure balance primary standard.

Solubility Measurement. The solute was loaded into a basket made of stainless-steel mesh, and was placed into the cell above the optical path. The cell was then purged with CO₂ to remove air, and sealed. The system was heated to the desired temperature, pressurized with CO₂ from a syringe pump, and the solution was allowed to equilibrate while being stirred. The cell was pressurized in 1 to 3 MPa increments over the range 10 to 25 MPa, with absorbance measurements made after attaining equilibrium at each pressure. Equilibration times were typically 15 to 30 minutes, although Tb(thd)₃ and Fe(thd)₃ required up to one hour to equilibrate. After constant absorbance was attained, spectra were measured in triplicate from 1300 to 2500 nm. At all pressures, the background absorbance from CO₂ in the quantitative region was less than the standard deviation of replicate measurements. Therefore, no background corrections were necessary.

Calibration. All calibration standards were prepared by adding a known amount of the metal chelate to the cell, heating the cell, and pressurizing the contents with CO₂ until the absorbance of the peak maximum (λ_{max}) remained constant with the addition of CO₂. The absorbance was calculated by subtracting the baseline absorbance value at 1518 nm from the absorbance at λ_{max} (Table 1). Each standard was measured in triplicate and Beer-Lambert Law plots were attained with correlation coefficients (R^2) of 0.9970 to 0.9998.

Extraction Apparatus and Method. The extraction apparatus consisted of a high-pressure syringe pump and an oven containing two PEEK vessels and an exit valve. Upon entering the oven, the CO₂ was heated in a coil (1 m) of stainless steel tubing. With the exception of this coil, all tubing used in the system was 0.16 cm PEEK. CO₂ first entered a 0.8 mL vessel containing a 100-fold excess of H(tod), with respect to the metal ion, where CO₂ was saturated with the chelating agent. The supercritical CO₂ then percolated through 4 mL of an aqueous or sodium acetate (100 mM or 3 M) solution containing 100 µg of a given metal ion contained within a 7.9 mL extraction vessel. The solution was first extracted statically for 15 minutes and then dynamically for 20 minutes with a CO₂ flow rate of 3.0 mL/min. For both stages of the extraction, the CO₂ was maintained at 333 K and 20.3 MPa. The extracted chelate was collected in methanol following depressurization through a 63.5 µm i.d. PEEK restrictor. The extraction efficiency was determined by analyzing the metal content remaining in the aqueous solutions by inductively coupled plasma atomic emission spectroscopy. Each extraction was performed a minimum of three times with a typical standard deviation of $\pm 10\%$.

Results and Discussion

Solubility Measurement. The concentration of a given metal chelate in supercritical CO₂ was determined using the Beer-Lambert Law. Two NIR regions were available for analysis; the first overtone region of the C-H stretching vibration (1650 to 1800 nm) and the more intense combination band region (2250 to 2500 nm). We used the

overtone region to quantify the solubility of the more soluble chelates, and the combination region for the less soluble chelates.

Molar absorptivity coefficients, ϵ , for the metal chelates are listed in Table 1. For hydrocarbons, ϵ has been shown to be pressure dependent in UV-visible and IR spectroscopy;^{6, 10} however, others have found very little change in ϵ with increasing pressure or temperature using NIR spectroscopy.¹¹ We also found ϵ to be independent of pressure and temperature for the chelates studied. Nine replicate measurements of ϵ for five different concentrations of Ce(tod)₄ at 323 and 333 K gave an average relative standard deviation of 0.9 % over the pressure range 16.2 to 32.2 MPa. All uncertainties reported herein include a coverage factor, $k = 2$.¹² Moreover, we did not observe a shift in λ_{max} over the range of these measurements.

While several researchers have used NIR to determine the solubility of organic compounds in supercritical fluids, this is the first study of metal chelate solubility by NIR. To check the accuracy of the NIR static method, the solubility of Fe(acac)₃ was measured in CO₂ and compared to the Fe(acac)₃ solubility isotherm at 313 K obtained by Lagalante¹³ using a UV-visible static method.¹⁴ The two data sets are shown in Figure 2. There is good agreement between the two data sets at lower densities; however, at the highest density measured, the UV-visible solubility is 1.6 times higher than the NIR. As the UV-visible data was calibrated to liquid solvent standards, the differences between these data sets falls within the range observed by Rice.⁶ The reproducibility of two replicate NIR measurements for Fe(acac)₃ at 313 K was $\pm 1.8\%$, comparable to the experimental uncertainty of the UV-visible method ($\pm 2.0\%$).

Tables 2-5 summarize the measured solubility of the complexes in mole fraction, y , and solubility, S (g/L), as a function of CO₂ density. In these experiments, the density was calculated at the experimental temperature and pressure of pure CO₂.¹⁵ For the more soluble chelates, however, the large quantity of solute dissolved in CO₂ is expected to cause a discrepancy between the actual and calculated density. Solubility data are expressed with an average relative standard deviation of 5.1 % based on two to three separate measurements of the 313, 323, and 333 K isotherms of Tb(tod)₃. Compared with literature solubility data,^{4, 5} Ce(tod)₄, Tb(tod)₃, Fe(tod)₃, and Fe(thd)₃ are among the most soluble metal chelates studied to date, including the CO₂-philic fluorinated metal chelates.

Ce(tod)₄ and Tb(tod)₃ are an order of magnitude more soluble than Ce(thd)₄ and Tb(thd)₃. We have recently determined the crystal structures of the tod chelates and found that tod forms a more compact ligand shell around Ce⁴⁺ and Tb³⁺ than does thd.⁸ Although tod and thd are isomers, thd is sterically rigid, while the isobutyl group of tod is more flexible. Better shielding of the highly charged Ce⁴⁺ and Tb³⁺ by tod increases the lipophilicity and solubility of the tod chelates in non-polar supercritical CO₂. These measurements indicate that β -diketonates containing isobutyl groups can be more CO₂-philic than those with *tert*-butyl groups in facilitating solubility in supercritical CO₂.

Although Fe(tod)₃ is more soluble than Fe(thd)₃, the solubility difference between these chelates is not as great as in the case above. It is likely that the smaller ionic radius of Fe³⁺ compared to Ce⁴⁺ and Tb³⁺ lessens the distinction between tod and thd in terms of metal shielding. Nonetheless, the isobutyl group functions at least as well as the *tert*-butyl

group even for first row transition metal chelates. By contrast, the smaller acac ligand is unable to effectively shield Fe^{3+} , and $\text{Fe}(\text{acac})_3$ has very low solubility.

Terbium Chelates. To determine whether the terbium chelates were present as the dimer or monomer in supercritical CO_2 , we measured the infrared spectrum of each chelate in CO_2 from 313 to 333 K and 10 to 20 MPa. $\text{Tb}_2(\text{tod})_6$ or $\text{Tb}_2(\text{thd})_6$ was loaded into a high-pressure IR cell,¹⁶ the cell was sealed, heated, and charged with CO_2 to a set pressure. Under all conditions, the characteristic Tb-O-Tb stretch of the dimer was absent from the IR spectra, indicating that only the monomers, $\text{Tb}(\text{tod})_3$ and $\text{Tb}(\text{thd})_3$, were present in supercritical CO_2 .⁸

Correlation of Experimental Solubility Data. The experimental solubility data for the metal chelates were correlated using the empirical model proposed by Chrastil:⁷

$$S = \rho^k \exp(a/T + b), \quad (1)$$

where S is the solubility (g/L) of the metal chelate dissolved in supercritical CO_2 , ρ is the density (g/L) of pure CO_2 at the experimental temperature and pressure, k is the number of CO_2 molecules associated with the metal chelate, $a = \Delta H/R$ (where ΔH is the sum of the enthalpies of vaporization and solvation), and b is a constant. By performing a multiple linear regression on $\ln S$ as a function of $\ln \rho$ and $1/T$, the coefficients k , a , and b are obtained. These coefficients are listed in Table 6 along with ΔH calculated from a . Representative plots of $\ln S$ vs. $\ln \rho$ are shown for the tod chelates in Figure 3 along with the best-fit line using equation 1.

Smart and coworkers have recently reviewed available metal chelate solubility data and correlated this data to the model of Chrastil in an effort to compile and predict

solubilities in supercritical CO₂.⁴ While this correlation is by no means a rigorous method for quantifying intermolecular associations or metal chelate vapor pressures, it does provide a way to compare metal chelate solubilities over a range of densities. For the metal chelates studied, the association number, k , ranges from approximately three to seven CO₂ molecules, within the range computed by Smart.⁴ Although k is expected to depend on density, equation 1 predicts a linear relationship between $\ln S$ vs. $\ln \rho$ with a slope of k . Deviations from linearity in fitting equation 1 to the experimental data may arise from potential discrepancies between the actual and calculated densities for the highly soluble chelates. In the Chrastil model, ΔH represents the sum of the enthalpy of vaporization and the enthalpy of solvation. Within the series of tod and thd chelates, ΔH increases with increasing solubility, e.g., Fe(tod)₃, Ce(tod)₄ and Tb(tod)₃ have $\Delta H = -15.24$, -22.59 , and -64.29 kJ/mol respectively. This may simply be the effect of solubility increasing with increased vapor pressure (increased enthalpy of vaporization) although there is not enough thermodynamic data available for these chelates to make definite conclusions.

Extraction Data. Aqueous and sodium acetate solutions containing 25 ppm Ce⁴⁺, Tb³⁺, or Fe³⁺ were extracted using H(tod) and supercritical CO₂ at 333 K and 20.3 MPa (Table 7). Because unbuffered water in contact with supercritical CO₂ has a pH of 2.9,¹⁷ sodium acetate solutions were used to cause deprotonation of H(tod) (estimated pKa of 11.1).¹⁸ While basic solutions favor the deprotonation of H(tod), metal ions form insoluble hydroxides at higher pH values, which can in some instances impede the extraction. The apparent extraction efficiencies of 38 to 76 % observed for Ce⁴⁺, Tb³⁺, and Fe³⁺ demonstrate the potential of this method, although optimization of pH conditions, the

addition of a mixing device, and repetitive extractions would all likely improve the efficiencies.

Conclusions

The supercritical carbon dioxide solubilities of the β -diketonate complexes Ce(tod)₄, Ce(thd)₄, Tb(tod)₃, Tb(thd)₃, Fe(tod)₃, Fe(thd)₃, and Fe(acac)₃ were measured using near infrared spectroscopy from 313 to 333 K and 10 to 35 MPa. The resulting solubility isotherms for the metal chelates showed linear behavior versus CO₂ density in a log-log plot. Solubilities of the tod chelates are in all cases higher than the thd and acac chelates. The increased flexibility of the isobutyl substituent on tod appears to enhance the shielding of the metal center and may be responsible for the order of magnitude increase in the solubilities of Ce(tod)₄ and Tb(tod)₃ over those of Ce(thd)₄ and Tb(thd)₃. The Chrastil model correlated the experimental data with average absolute relative deviations of 6.2 to 20.0%. H(tod) shows potential as an inexpensive chelating agent for SFE with 38, 76, and 68 % metal removed from aqueous solutions for Ce⁴⁺, Tb³⁺, and Fe³⁺, respectively.

Acknowledgements

WCA is grateful to the U.S. EPA and CIRES Graduate Fellowship Programs for financial support, to J. Wells and T. W. Randolph for the use of their high-pressure infrared cell, and to F. Luiszer for ICP-AES analysis.

Literature Cited

- (1) Wai, C. M.; Wang, S. Supercritical Fluid Extraction: Metals as Complexes. *J. Chromatog., A* **1997**, 785, 369-383.
- (2) Ashraf-Khorassani, M.; Combs, M. T.; Taylor, L. T. Supercritical Fluid Extraction of Metal Ions and Metal Chelates from Different Environments. *J. Chromatog., A* **1997**, 774, 37-49.
- (3) Burford, M. D.; Ozel, M. Z.; Clifford, A. A.; Bartle, K. D.; Lin, Y.; Wai, C. M.; Smart, N. G. Extraction and Recovery of Metals Using a Supercritical Fluid with Chelating Agents. *Analyst* **1999**, 124, 609-614.
- (4) Smart, N. G.; Carleson, T.; Kast, T.; Clifford, A. A.; Burford, M. D.; Wai, C. M. Solubility of Chelating Agents and Metal-Containing Compounds in Supercritical Fluid Carbon Dioxide. *Talanta* **1997**, 44, 137-150.
- (5) Darr, J. A.; Poliakoff, M. New Directions in Inorganic and Metal-Organic Coordination Chemistry. *Chem. Rev.* **1999**, 99, 495-542.
- (6) Rice, J. K.; Niemeyer, E. D.; Bright, F. V. Evidence for Density-Dependent Changes in Solute Molar Absorptivities in Supercritical CO₂: Impact on Solubility Determination Practices. *Anal. Chem.* **1995**, 67, 4354-4357.
- (7) Chrastil, J. Solubility of Solids and Liquids in Supercritical Gases. *J. Phys. Chem.* **1982**, 86, 3016-3021.
- (8) Andersen, W. C.; Noll, B. C.; Sellers, S. P.; Whildin, L. L.; Sievers, R. E. Characterization and Structures of the 2,2,7-Trimethyl-3,5-Octanedionate Chelates of Cerium(IV) and Terbium(III). *Submitted to Inorg. Chem.* **2000**.

- (9) Wenzel, T. J.; Williams, E. J.; Haltiwanger, R. C.; Sievers, R. E. Studies of Metal Chelates with the Novel Ligand 2,2,7-Trimethyl-3,5-Octanedione. *Polyhedron* **1985**, *4*, 369-378.
- (10) Inomata, H.; Yagi, Y.; Saito, M.; Saito, S. Density Dependence of the Molar Absorption Coefficient - Application of the Beer-Lambert Law to Supercritical CO₂ - Naphthalene Mixture. *J. Supercrit. Fluids* **1993**, *6*, 237-240.
- (11) Swaid, I.; Nickel, D.; Schneider, G. M. NIR-Spectroscopic Investigations on Phase Behaviour of Low-Volatile Organic Substances in Supercritical Carbon Dioxide. *Fluid Phase Equilib.* **1985**, *21*, 95-112.
- (12) Taylor, B. N.; Kuyatt, C. E. *Guidelines for Evaluating and Expressing the Uncertainty of NIST Measurement Results*; Tech. Note 1297; National Institute of Standards and Technology: Washington, DC, 1994.
- (13) Lagalante, A. F. The Measurement, Modeling, and Applications of Metal β -Diketonate Complexes Dissolved in Supercritical Carbon Dioxide. Ph.D. Thesis, University of Colorado, Boulder, 1995.
- (14) Lagalante, A. F.; Hansen, B. N.; Bruno, T. J.; Sievers, R. E. Solubilities of Copper(II) and Chromium(III) β -Diketonates in Supercritical Carbon Dioxide. *Inorg. Chem.* **1995**, *34*, 5781-5785.
- (15) Span, R.; Wagner, W. A New Equation of State for Carbon Dioxide Covering the Fluid Region from the Triple-Point Temperature to 1100 K at Pressures up to 800 MPa. *J. Phys. Chem. Ref. Data* **1996**, *25*, 1509-1596.

- (16) Designed by J. Webb and T. W. Randolph. Department of Chemical Engineering, University of Colorado, Boulder, CO 80309-0424.
- (17) Toews, K. L.; Shroll, R. M.; Wai, C. M.; Smart, N. G. pH-Defining Equilibrium between Water and Supercritical CO₂. Influence on SFE of Organics and Metal Chelates. *Anal. Chem.* **1995**, 67, 4040-4043.
- (18) Andersen, W. C. Solubility and Extraction of Cerium(IV), Terbium(III), and Iron(III) β -Diketonates in Supercritical Carbon Dioxide. Ph.D. Thesis, University of Colorado, Boulder, 2000.

Tables and Figures

Table 1. Molar absorptivity and absorbance maxima of metal chelates in supercritical CO₂

Metal Chelate	ϵ (L•mol ⁻¹ •cm ⁻¹)	λ_{max} (nm)
Ce(tod) ₄	2.43 \pm 0.07	1696
Tb(tod) ₃	1.67 \pm 0.03	1696
Fe(tod) ₃	1.73 \pm 0.03	1696
Ce(thd) ₄	19.0 \pm 1.8	2308
Tb(thd) ₃	6.71 \pm 0.14	2306
Fe(thd) ₃	1.97 \pm 0.03	1694
Fe(acac) ₃	4.09 \pm 0.12	2264

Table 2. Solubilities of Ce(tod)₄ and Ce(thd)₄ in supercritical carbon dioxide

Ce(tod) ₄				Ce(thd) ₄			
<i>P</i> (MPa)	ρ (g/L)	$10^3 y$	<i>S</i> (g/L)	<i>P</i> (MPa)	ρ (g/L)	$10^3 y$	<i>S</i> (g/L)
<i>T</i> = 333 K							
14.54	587.6	1.67	19.45	13.31	525.1	0.05	0.49
16.82	662.5	2.99	39.44	15.29	616.9	0.11	1.38
18.60	701.2	4.22	58.92	17.62	681.3	0.23	3.15
21.46	746.4	6.08	90.61	19.68	720.2	0.32	4.63
				22.27	757.0	0.42	6.23
				25.29	790.2	0.50	7.90
				27.88	813.5	0.55	8.92
				30.60	834.4	0.59	9.80
				34.59	860.7	0.62	10.58
<i>T</i> = 323 K							
12.54	616.6	1.63	19.97	11.77	569.8	0.06	0.65
12.82	630.3	2.00	25.05	12.40	609.3	0.08	0.96
14.84	697.8	3.09	42.92	14.18	680.0	0.14	1.86
17.89	756.8	4.63	69.79	16.21	728.1	0.20	2.88
19.99	785.2	6.22	97.53	18.29	762.8	0.25	3.84
24.30	828.8	7.84	129.95	20.31	789.0	0.30	4.66
				23.03	817.4	0.34	5.59
				25.94	842.3	0.38	6.38

				28.56	861.4	0.41	7.05
				31.68	881.2	0.44	7.64
				34.75	898.3	0.45	8.02
$T = 313 \text{ K}$							
9.80	611.8	1.53	18.57	10.12	637.7	0.05	0.65
10.43	657.4	1.87	24.44	12.38	729.2	0.10	1.51
12.19	724.7	2.78	40.11	14.42	772.0	0.14	2.19
14.53	773.7	3.95	60.94	16.49	802.4	0.17	2.79
16.93	807.9	4.07	65.56	18.50	825.7	0.20	3.29
				21.44	862.1	0.23	3.85
				24.13	874.1	0.25	4.28
				27.08	893.6	0.26	4.61
				29.87	909.8	0.27	4.87
				32.68	924.4	0.28	5.08
				35.09	935.8	0.29	5.17

Table 3. Solubilities of Tb(tod)₃ and Tb(thd)₃ in supercritical carbon dioxide

Tb(tod) ₃				Tb(thd) ₃			
<i>P</i> (MPa)	ρ (g/L)	10^3 <i>y</i>	<i>S</i> (g/L)	<i>P</i> (MPa)	ρ (g/L)	10^3 <i>y</i>	<i>S</i> (g/L)
<i>T</i> = 333 K							
14.06	565.8	0.55	5.01	17.21	671.9	0.28	3.07
14.80	598.3	0.78	7.51	20.73	736.3	0.30	3.52
15.31	617.7	0.88	8.74	23.40	770.3	0.32	4.02
16.76	661.0	1.37	14.61	28.08	815.0	0.34	4.50
17.34	675.0	1.50	16.30	34.97	862.9	0.34	4.73
18.94	707.5	2.12	24.20				
19.58	718.5	2.26	26.26				
20.84	737.9	2.84	33.84				
21.29	744.1	2.79	33.50				
23.67	773.3	3.45	43.11				
<i>T</i> = 323 K							
12.83	630.4	0.53	5.41	12.46	612.7	0.10	1.02
14.65	692.9	1.19	13.34	14.60	691.7	0.15	1.63
14.68	693.7	1.26	14.06	16.53	734.1	0.17	2.01
14.92	699.8	1.08	12.15	18.76	771.2	0.19	2.34
16.57	734.9	1.84	21.80	20.64	792.8	0.20	2.58
16.82	739.3	1.61	19.18	23.71	823.7	0.23	2.99
18.74	769.1	2.52	31.27	26.74	848.4	0.23	3.18

18.96	772.0	2.07	25.77	30.04	871.1	0.24	3.34
20.80	794.6	2.87	36.83	35.23	900.8	0.24	3.48
20.95	796.2	2.41	30.99				
22.57	813.0	3.17	41.68				
23.88	825.2	3.40	45.39				
26.58	847.2	3.72	50.91				
$T = 313 \text{ K}$							
12.43	731.0	0.64	7.60	12.46	731.7	0.07	0.88
14.54	774.0	0.87	10.90	15.14	783.6	0.09	1.17
14.98	781.0	0.97	12.20	18.58	826.6	0.11	1.46
16.49	802.4	1.06	13.67	23.39	868.7	0.12	1.70
16.62	804.1	1.15	14.85	30.38	912.5	0.15	2.15
18.77	828.5	1.24	16.52				
20.52	845.3	1.43	19.53				
21.54	854.1	1.40	19.35				
24.83	879.0	1.53	21.74				
25.12	881.0	1.62	23.07				
30.56	913.5	1.64	24.14				
31.84	920.2	1.72	25.48				

Table 4. Solubilities of Fe(tod)₃ and Fe(thd)₃ in supercritical carbon dioxide

Fe(tod) ₃				Fe(thd) ₃			
<i>P</i> (MPa)	ρ (g/L)	$10^3 y$	<i>S</i> (g/L)	<i>P</i> (MPa)	ρ (g/L)	$10^3 y$	<i>S</i> (g/L)
<i>T</i> = 333 K							
13.11	513.1	1.55	10.97	13.88	556.8	3.91	30.10
14.46	584.2	3.71	29.96	14.22	573.3	4.70	37.29
15.23	614.7	5.02	42.64	15.71	630.9	8.70	76.16
15.90	636.9	6.82	60.19	16.30	648.6	7.88	70.91
16.18	645.2	7.75	69.38	18.48	698.8	10.13	98.40
16.63	657.5	8.60	78.53				
17.74	683.8	12.67	120.80				
<i>T</i> = 323 K							
11.10	512.1	1.39	9.83	12.27	602.1	2.99	24.82
12.46	612.6	4.13	35.00	14.44	687.2	3.72	35.35
12.79	629.0	4.75	41.30	17.25	746.6	4.34	44.79
13.91	671.6	6.20	57.71	20.20	787.7	4.69	51.05
14.47	688.1	8.25	78.75	24.37	829.4	4.82	55.29
16.50	733.6	10.30	105.07	30.67	875.0	5.85	70.85
<i>T</i> = 313 K							
9.06	498.2	1.75	12.03	9.48	575.0	1.64	13.01
9.31	548.2	2.64	19.93	10.40	655.9	2.30	20.83
10.75	673.9	5.48	51.09	12.36	729.0	3.40	34.19

11.28	695.9	6.48	62.50	14.54	774.0	4.24	45.38
12.16	723.8	8.50	85.40	17.30	812.4	4.94	55.55
14.75	777.3	10.32	111.58	20.04	840.9	5.34	62.10
				24.15	874.2	5.60	67.78

Table 5. Solubility of $\text{Fe}(\text{acac})_3$ in supercritical carbon dioxide

$\text{Fe}(\text{acac})_3$			
$P(\text{MPa})$	$\rho(\text{g/L})$	$10^3 y$	$S(\text{g/L})$
$T = 333 \text{ K}$			
12.76	490.1	0.06	0.24
14.77	597.5	0.12	0.56
16.69	659.3	0.17	0.91
18.74	703.9	0.21	1.21
20.74	736.4	0.26	1.51
22.82	763.6	0.28	1.74
24.78	785.0	0.30	1.91
$T = 323 \text{ K}$			
11.99	585.1	0.07	0.32
12.68	623.6	0.06	0.31
13.46	656.4	0.10	0.55
14.75	695.6	0.09	0.51
16.31	730.1	0.13	0.74

16.35	730.8	0.13	0.75
17.00	742.5	0.11	0.65
18.33	763.3	0.14	0.84
18.96	772.1	0.13	0.80
20.56	791.9	0.15	0.92
21.25	799.5	0.14	0.92
22.89	816.1	0.16	1.04
23.80	824.5	0.15	1.02
24.92	834.1	0.17	1.14
24.99	834.7	0.18	1.19
26.55	847.0	0.17	1.14
27.13	851.3	0.19	1.29
29.65	868.6	0.19	1.36
29.67	868.8	0.18	1.28
32.36	885.2	0.20	1.39
33.40	891.0	0.19	1.36
34.86	898.9	0.20	1.46
$T = 313\text{K}$			
9.82	613.1	0.06	0.28
10.63	668.0	0.09	0.47
11.74	711.5	0.12	0.66
12.46	731.8	0.12	0.72

13.88	762.4	0.13	0.79
14.70	776.6	0.15	0.95
16.01	796.1	0.18	1.14
16.77	806.1	0.17	1.13
18.00	820.4	0.19	1.23
18.92	830.1	0.19	1.28
19.95	840.1	0.21	1.39
21.76	856.0	0.22	1.50
24.55	877.0	0.23	1.59
24.78	878.7	0.24	1.67
26.92	892.7	0.24	1.74
27.54	896.4	0.25	1.79
29.50	907.8	0.26	1.90
29.82	909.5	0.25	1.85
32.36	922.8	0.26	1.96
32.80	925.0	0.27	1.97
35.37	937.1	0.27	2.05

Table 6. Chrastil solubility coefficients from equation (1) and calculated enthalpies for metal chelates dissolved in supercritical CO₂

Compound	k	a	b	%AARD ^a	ΔH (kJ/mol)
Ce(tod) ₄	5.807 ± 0.235	-2717 ± 333	-25.83 ± 0.235	6.5	-22.59
Ce(thd) ₄	5.881 ± 0.145	-5882 ± 275	-19.60 ± 1.03	8.7	-48.90
Tb(tod) ₃	6.793 ± 0.352	-7733 ± 538	-18.09 ± 1.66	13.3	-64.29
Tb(thd) ₃	3.066 ± 0.199	-6432 ± 293	0.33 ± 1.41	6.2	-53.48
Fe(tod) ₃	6.070 ± 0.348	-1833 ± 542	-29.67 ± 2.59	13.5	-15.24
Fe(thd) ₃	3.218 ± 0.439	-5051 ± 827	-1.626 ± 2.82	20.0	-41.99
Fe(acac) ₃	3.873 ± 0.250	-1812 ± 512	-20.12 ± 1.72	18.8	-15.06

$$^a\%AARD = \frac{1}{N} \sum_{i=1}^N |(S_{\text{exp}} - S_{\text{calc}}) / S_{\text{exp}}| \times 100\%$$

Table 7. Ce⁴⁺, Tb³⁺, and Fe³⁺ remaining in aqueous solution after extraction with H(tod) and supercritical CO₂ at 333 K and 20.3 MPa

Matrix	% Remaining
(NH ₄) ₂ Ce(NO ₃) ₆ in unbuffered H ₂ O	62.3 ± 13.6
Tb(NO ₃) ₃ in 100 mM sodium acetate	23.6 ± 7.9
FeCl ₃ in unbuffered H ₂ O	48.8 ± 7.2
FeCl ₃ in 100 mM sodium acetate	48.4 ± 6.3
FeCl ₃ in 3 M sodium acetate	32.1 ± 10.6

Figure 1. High-pressure near infrared cell (left) and experimental set-up (right) (a) end fitting, (b) cell body, (c) sapphire window, (d) sample inlet port, (e) PEEK gaskets, (f) thermostat, (g) stir bar, (h) magnetic stirrer, (i) CO₂ cylinder, (j) high-pressure syringe pump, (k) near infrared spectrophotometer, (l) cell, (m) pressure transducer.

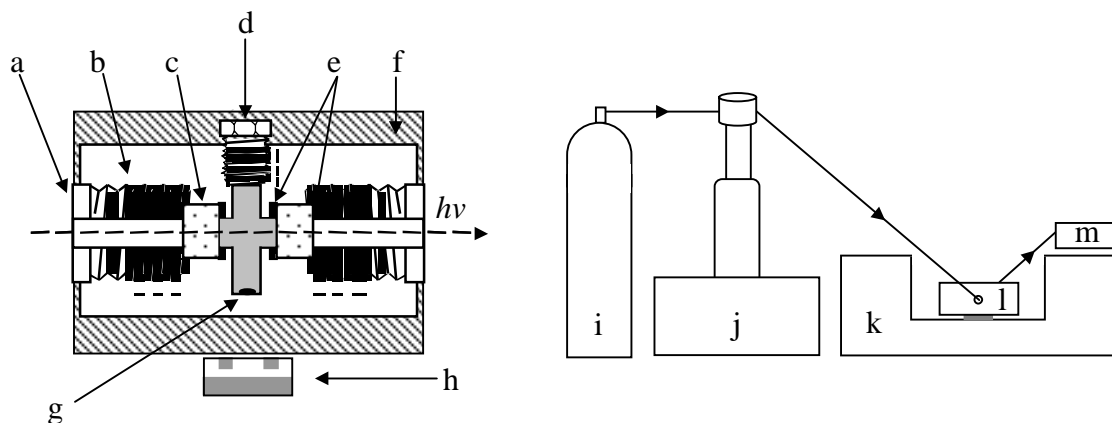


Figure 2. Solubility of Fe(acac)₃ in supercritical carbon dioxide at 313 K determined by NIR and UV-visible static methods.

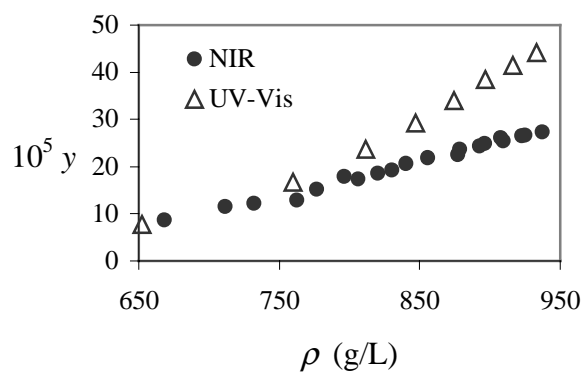


Figure 3. Solubility isotherms for (a) $\text{Ce}(\text{tod})_4$, (b) $\text{Tb}(\text{tod})_3$, and (c) $\text{Fe}(\text{tod})_3$ in supercritical carbon dioxide at 333 K (\star), 323 K (\boxtimes), and 313 K (π). Lines represent correlation by equation 1.

